Effects of Pore Additives on Deep Eutectic Solvent Immobilization for CO_2/N_2 Gas Separation Using Supported Deep Eutectic Solvent Membranes

Amira Mohd Nasib[a*], Nora Jullok[a,b] & Mohd Irfan Hatim Mohamad Dzahir[a,b],

[a]School of Bioprocess Engineering, Universiti Malaysia Perlis, Kompleks Pusat Pengajian Jejawi 3, 02600 Arau, Perlis, Malaysia
[b]Centre of Excellence BiomassUtilization, School of Bioprocess Engineering, Universiti Malaysia Perlis, Kompleks Pusat Pengajian Jejawi 3, 02600 Arau, Perlis, Malaysia

ABSTRACT

This work analyses the effect of two different pore additives focusing on polyethylene glycol (PEG) and lithium chloride (LiCl) at different concentrations on the immobilization of a deep eutectic solvent (DES) in a polyvinylidene fluoride-co-polytetrafluoroethylene (PVDF-co-PTFE) membrane. Two compounds were chosen to synthesized the DES; choline chloride as halide salt and ethylene glycol as a hydrogen bond donor. The DES was impregnated onto the membrane pores by applying a vacuum-based technique. The membranes were prepared via phase inversion by means of immersion precipitation. For characterization purposes, scanning electron microscopy (SEM-EDX) was used to analyse the morphology of the supported- DES-membranes together with energy dispersive X-ray spectrometry. The gravimetric method was applied to calculate the porosity, while the membrane performance for carbon dioxide (CO_2) permeation and separation was assessed to determine the capability of the DES-impregnated membrane. The outcomes demonstrating that the highest loading of DES in the membrane support was obtained when 3 wt% PEG was added into the polymer solution with a porosity of 70.5%. The CO_2 permeability and the CO_2/N_2 selectivity achieved using the synthesized membrane are 2.81×10^6 barrer and 3.46, respectively, when working with a transmembrane pressure of 1.1 bar and a temperature of 25°C at 200 cm^3 /min of gas flow rate. The results showed that additional of PEG as a pore additives able to load the highest DES in the membrane pore and resulted the best CO_2 permeability and the CO_2/N_2 selectivity.

Keywords: Pore additives, Gas separation, Membranes, PVDF

1.0 INTRODUCTION

Carbon dioxide (CO_2) is the main combustion product of solid waste and fossil fuels such as coal, natural gas and oil. At present, over 85% of the global energy demand is supplied by fossil fuels, where approximately 40% of the total CO_2 emission originated from fossil-fuelled power plants [1, 2]. Based on the Energy Information Agency report, it is expected that the power production plant from this type of fuel will increase by about 50% in the next 20 years due to the low cost and large domestic supply [3]. According to Merkel *et al*. (2010), the CO_2 concentration in the atmosphere has increased from 275 to 387 ppm during the last century [4]. The reading in 2017 was 405.0 ppm, which is clearly higher than the pre-industrial level of about 300 ppm [5].

The conventional technologies such as adsorption, absorption and cryogenic distillation were first to be introduced and have been used commercially to capture CO_2 from flue gas streams. However, due to several drawbacks such as secondary environmental effects, operational conditions and cost, membrane technology has widely used to replace the conventional technologies [6, 7]. The membrane technology has become the most common procedures used in the industries including water treatment, industrial water supply, chemical, pharmaceutical, biotechnological, beverages, food, metallurgy and other separation processes. Membrane technology now widely used is due to their excellent performance on combining selectivity and productivity, not changeable of the solute phase or the carrier solvent used, involved a relatively low energy use, ease of use, environmental friendly, and involving of none regeneration of liquid sorbents or solids [8-10]. The application of gas separation membrane on industrial scale was adapted by Permea (Air Products) in 1980. By the late 1980s, companies such as Cynara, UOP and Grace Membrane Systems started to develop commercial membrane plants for CO_2 separation. Since the 1990s, the use of membranes for CO_2 removal grew rapidly and have profited the companies of about $150 million/year [11]. As for this, Cellulose acetate (CA), polysulfone (PSf), polyimide (PI) and perfluoro polymers are widely selected polymers used commercially for CO_2 separation [12]. The range of applicable polymers is somehow still limited due to the factors amongst them involves of cost, difficult to process, and concentration polarization. In addition, polymeric membranes also have a trade-off between permeability and selectivity[13].

Supported liquid membranes (SLMs) are developed by impregnation of a selected liquid in the membrane matrix [14, 15]. The membrane act as a support to hold the liquid by capillary forces [16]. Scovazzo *et al.* (2002) pioneered research about SLMs, and incorporated ionic liquids (ILs) into the membrane pores for CO_2/N_2 gas separation. They noticed that high selectivity and flux were observed while using such supported ionic liquid membrane (SILM) as compared to conventional polymeric membranes [17]. Corresponding to reaction to SILM, ever since, ILs have been studied as attractive solvents due to their changeable physiochemical properties. Unfortunately, there are still some challenges to be addressed, such as their low sustainability, biocompatibility and biodegradability [18]. This is whereby another option could be to adopted as a deep eutectic solvent (DES) is used as an alternative to the ILs.

A DES is a liquid that consists of two or three environmentally friendly components that have an ability of self-association. The selected components formed a eutectic mixture through hydrogen bond interactions. In general, a DES is synthesized by adding a quaternary ammonium salt (or known as hydrogen bond acceptor, HBA) with a hydrogen bond donor (HBD) such as metal salt, which has an ability to form a complex with the halide anion of the quaternary ammonium salt [19]. A DES indeed, might become a suitable solvent to replace the traditional ionic liquids (ILs) which can be easily prepared with high purity at low cost and environmentally friendly while having similar physical-chemical properties as ILs [20, 38].

In this study, the effect of additional pore additives such as PEG and LiCl on membrane porosity is investigated, as to study the DES loading on different membrane microstructures, and to evaluate the membrane performance in CO_2/N_2 gas separation.

2.0 MATERIALS AND METHODS

Poly(vinylidene fluoride-co-tetrafluoroethylene) (PVDF-co-PTFE) was obtained from Arkema Pte Ltd, Singapore. Choline chloride (ChCl) (≥ 99.0% purity), which is commonly used additives for animal feeds are abundantly available. However, in this experiment, ChCl and polyethylene glycol (PEG) (≥ 99.0% purity) with average of MW 10,000 and reagent grade is used and were acquired from Sigma Aldrich. N-dimethylacetamide (DMAc) and ethylene glycol were obtained from Merck Milipore Corporation with ≥ 99.0% purity, while Lithium chloride, LiCl (≥ 99.0% purity) was obtained from Fisher Scientific.

2.1 Synthesis of Microstructured Membranes by Phase Inversion Method

PVDF-co-PTFE polymer at 20 wt % was added to a predetermined weight of DMAc as solvent to prepare a homogeneous polymer solution. The appropriate amount of additive (LiCl or PEG) was slowly added and stirred uninterruptedly at a speed of 200 rpm until the solution became homogeneous and clear. Throughout the stirring process, the temperature was kept constant at 50±5 °C. Then, the homogeneous polymer solution was aerated for 24 hours at ambient temperature. The aeration step was done to ensure all the bubbles were removed before membrane casting was done. The solution was placed in a desiccator and attached with a vacuum pump. The vacuum pump was left on until the bubbles disappearing. Table 1 summarizes the types of membrane used in this study based on different DMAc: PEG: LiCl ratios.

Table 1 Types of synthesized membrane based on different in chemical ratios

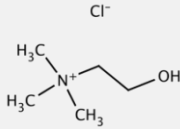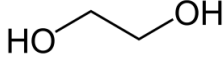| DMAc (wt %)	PEG (wt %)	LiCl (wt %)	Membrane
80	-	-	M-0
79	1	-	M-P1
78	2	-	M-P2
77	3	-	M-P3
79	-	1	M-L1
78	-	2	M-L2
77	-	3	M-L3

*Weight of PVDF-co-PTFE polymer was fixed throughout the experiment at 20 wt %.

PVDF-co-PTFE flat sheet membranes were synthesized via non-solvent induced phase separation (NIPS). The polymer solution was hand-cast on the glass plate using a hand-casting knife. A 400±10 μm knife gap was set for casting purposes. The casted film was left in ambient air approximately for 30 seconds before been immersed into a coagulation bath using pure distilled water for 24 hours. The flat sheet membrane film was then removed from the coagulation bath before being dried at room temperature for 24 hours [21].

2.2 Synthesis of Deep Eutectic Solvent (DES)

The DES used was first synthesised by mixing ethylene glycol and ChCl at room temperature by using a ratio of 1:3. The selected components formed a eutectic mixture through hydrogen bond interactions. The solution was stirred rapidly at speeds of 200 rpm until its reach a homogeneous and clear solution was observed. Table 2 shows the properties of ChCl and ethylene glyco.

Table 2 Properties of choline chloride and ethylene glycol [22]

Chemicals	Choline chloride	Ethylene Glycol
Chemical Formula		
Boiling Point, °C	-	197.6
Melting Point, °C	302 to 305	-14 to -10
Molecular weight, g/mol	139.62	62.07
Density (g/cm^3)	1.10	1.11
Viscosity (mPa.s)	21.0	21

2.3 Preparation of Supported Deep Eutectic Solvent Membranes

Vacuum immobilization was applied to prepare a supported deep eutectic solvent membrane. By using a Petri dish, the sample membranes were submerged into the DES and placed in a desiccator with a constant pressure of 10 mbar by using a vacuum pump for 3 hours at room temperature. At every hour, the desiccator was aerated to ensure the membrane pores were filled with DES. By using a filter paper, the excess of DES on the membrane surface was cleaned and removed.

2.4 Membrane Coating

The impregnated membrane was submerged into a solution containing PDMS/n-hexane at 3 wt% for 10 minutes to ensure the membrane pinholes were covered. Then, the sample membrane was cured for 24 hours at room temperature.

2.5 Membrane Characterization

2.5.1 *Analysis of Membrane Morphology and Micropores Determination*

A scanning electron microscope (SEM) of model JSM 6260 LE JEOL was used to study cross-sectional analysis and top surface morphologies of the prepared membrane. The membrane pore sizes were observed in the SEM micrographs and the diameter of the pores was measured by using ImageJ software.

2.5.2 *Porosity Measurement*

In this study, octanol was used to analyse the porosity of the prepared membrane. The membrane samples were immersed in octanol for 2 minutes and then dried by using a filter paper. The mass difference between the initial membrane and the same membrane after immersion in octanol was recorded. The membrane porosity was calculated by using Equation (1).

$$\omega = \frac{m_n/\rho_n}{m_n/\rho_n + m_p/\rho_p} \times 100 \tag{1}$$

where ω is the membrane porosity, m_n is the mass of absorbed octanol, m_p is the mass of dry membrane, ρ_n is the density of octanol and ρ_p is the density of the membrane. This method is used to estimate the porosity by determining the weight of the liquid contained in the membrane pores [23-25].

2.5.3 *Gas Permeation Test*

The performance of the synthesised membrane was tested by using a single gas permeation test. The ideal gas permeability was determined at a

constant gas flow rate of 200 cm³/min. The membrane was mounted onto the membrane cell with an effective area of 11.34 cm². The active layer of the membrane was placed by facing to the feed gas of pure CO_2 or N_2, respectively. The transmembrane pressure was kept constant at 1.1 bar and at temperature of 25 ºC±1. The ideal permeability of a gas i, (P_i) was calculated using Equation (2):

$$(P_i) = \frac{Q_i.l}{A(\Delta p)} \qquad (2)$$

where i represents the gas penetrant, Q_i is the volumetric flow rate of the gas i permeating through the membrane at standard temperature and pressure (cm³/s, (STP)). The gas flow rate was controlled by the flow meter, l is the thickness of the membrane (cm), A is the effective membrane area (cm²) and Δp is the transmembrane pressure drop (cmHg). The permeability is expressed in Barrer using below conversion.

$$1 \; Barrer = 1 \times 10^{-10} \frac{cm^3(STP).cm}{cm^2.S.cmHg}$$

The CO_2/N_2 selectivity was obtained by Equation (3):

$$\alpha_{(CO_2/N_2)} = \frac{P_{CO_2}}{P_{N_2}} \qquad (3)$$

where $\alpha_{(CO_2/N_2)}$ is the selectivity of CO_2 over N_2. Both P_{CO_2} and P_{N_2} represent the permeability of CO_2 and N_2, respectively.

2.5.4   Sample Analyses

The membranes thickness and pore size were measured from SEM images by using ImageJ software. Approximately,

10 measurements were taken for each sample to obtain the average value.

3.0 RESULTS AND DISCUSSION

3.1 Effect of Pore Additives on the Membrane Structure

SEM images of the membrane top surface and cross-sectional area of synthesised membranes are illustrated in Figure 1. It is suggested that the membrane top surface morphology of M-0 (Figure 1A) shows there are almost a smooth surface with no clear pores formation when no additive was used. However, it is observed there were pinholes that existed due to the tiny air bubbles that trapped in the polymer solution prior to membrane casting. The cross-sectional area of the same membrane shows a finger-like structure with dominant macrovoids. From scanning electron micrographs of prepared PVDF-co-PTFE membranes, it can be seen that by adding non-solvent pore additives into the polymer solution, the membrane morphology can be altered. Figure 1A (M-P1) indicates a membrane with pores on top of the membrane surface, which shows that the addition of PEG promotes for pore formation. The quantity of pores increases as the PEG percentage increases from 1 wt % to 3 wt %. As illustrated in Figure 1B; M-P1, M-P2 and M-P3, it is observed that the membrane cross sectional area has a similar pattern. It is also suggesting that the size of the macrovoids increases as the PEG quantity increases. Comparatively, when LiCl was used as a pore additive, less geometrical patent on pore is obtained (as illustrated in Figure 1B of M-L1, M-L2 and M-L3). After all, membrane with LiCl showed a dominant form of sponge-like structure as compared to the membrane with PEG with finger-like structure. In Figure 1A (M-L1), it shows a membrane with 1

wt % of LiCl that appears of a honeycomb-like structure with vague form of pores. Consistently, by increasing the LiCl amount, it leads to a clearer pore formation. As can be seen, all membranes in which LiCl was used as a pore additive, it consists of typical asymmetric pattern structure of three significant configurations; (i) top layer, (ii) finger-like, and (iii) sponge-like sub-layer. The finger-like layer diminished with less dosage of LiCl, while the sponge-like layer increased as the LiCl dosage increased.

The study conducted by Aroon *et al.* (2010) deduced that the use of a suitable pore additive into the polymer solution can actually shorten the precipitation path and accelerate the coagulation process. Hence, they discovered that those membranes appeared with more uniform structure with suitable pore additives [26]. In fact, PEG is categorized as a polymeric additive, while LiCl is known as a low molecular weight inorganic salt. Both additives were found to suppress the macrovoid development, however, LiCl was observed has a greater significant effect as compared to PEG as additive. This is shown in Table 2, in which the membrane pores size was found to be significantly different. A membrane with LiCl shows a smaller pore size compared to a membrane with PEG as additive. LiCl in the polymer solution reduced macrovoid formation (as in kinetic effect) as the concentration increases. This can be explained by the high viscosity of the polymer solution containing LiCl due to the formation of acid-base complexes between LiCl and DMAc [27].

In the previous study, they discovered that the critical factors that affected the membrane performance in gas separation always liaised to the membrane porosity [28]. Table 2 shows the physical properties of the fabricated PVDF-co-PTFE membranes. It is observed that the membrane porosity increases with the PEG mass fraction (M-P3 > M-P2 > M-P1 > M-0). A similar trend was noticed in a study carried out by Alamery et. al (2016) where additional PEG in the polymer solution increased the porosity of a Poly(vinylidene fluoride-co-hexafluoropropylene) (PVDF-co-HFP membrane [29]. On the contrary, a membrane with LiCl as a pore additive shows a decrement in porosity as well as in membrane thickness. This can be explained in the changes of membrane morphology from a finger-like structure to a sponge-like structure as the percentage of LiCl increased [30].
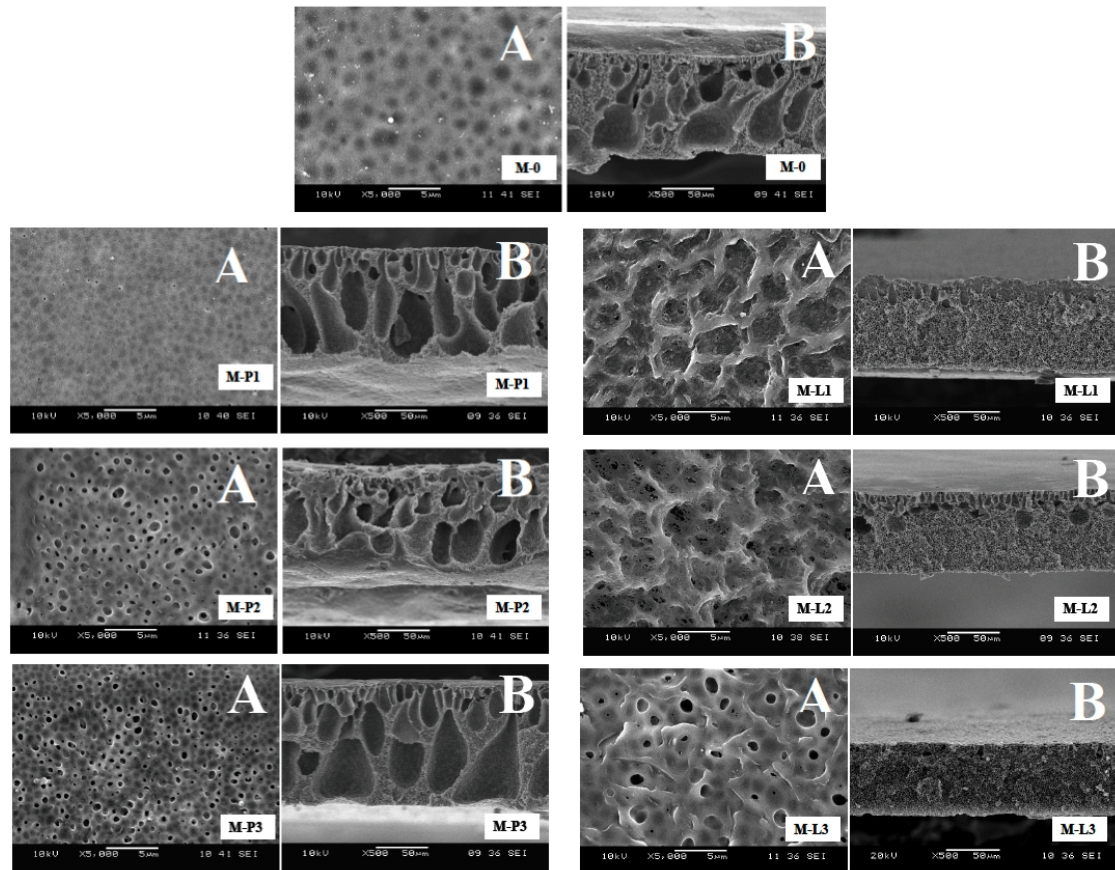
Figure 1 Scanning electron micrographs of prepared PVDF-co-PTFE membrane (A) top surface and (B) cross sectional area with different pore additives

Table 2 Porosity, pore size and thickness of fabricated PVDF-co-PTFE

Membrane	Porosity (%)	Pore Size (μm)		Thickness (μm)
		Minimum	Maximum	
M-0	56.1 ± 2.3	0.4 ± 0.06	46.9 ± 5.1	98.6 ± 2.3
M-P1	58.6 ± 3.3	0.4 ± 0.04	39.7 ± 4.5	103.9 ± 1.8
M-P2	68.5 ± 4.1	0.3 ± 0.05	30.8 ± 2.3	96.7 ± 3.1
M-P3	70.5 ± 2.3	0.6 ± 0.08	35.0 ± 3.6	114.0 ± 1.5
M-L1	64.1 ± 1.7	0.5 ± 0.03	18.7 ± 1.2	86.6 ± 2.4
M-L2	61.0 ± 2.3	0.5± 0.02	8.4 ± 0.6	74.0 ± 3.9
M-L3	55.9 ± 1.9	0.5± 0.01	5.5 ± 0.5	67.0 ± 4.6

3.2 Effect of Pore Additives on the Loading of Deep Eutectic Solvents

SEM-EDX analysis was used to confirm the presence of liquid impregnated in the matrix membrane by detecting the DES elements. The analysis results for supported-DES membranes are summarised in Table 3. Fluorine and carbon were amongst the dominant elements for the membrane supports, as illustrated in the PVDF-co-PTFE polymer chain. In fact, chlorine, nitrogen and oxygen were used to represent the DES, and silicone represents PDMS coating. Table 3 highlights the increment of DES loading in the membrane support as the percentage of PEG increased from 1 to 3 wt%. The DES loading increases as the

membrane porosity increases from 58.6 to 70.5 %;as the M-P3 membrane has the highest DES loading. The presence of macrovoids in M-P3 with a size of 0.60 to 35.0 μm (minimum and maximum pore sizes) assisted the membrane support to retain the highest amount of DES. Furthermore, with higher pore formation on top of the M-P3 membrane surface, it allowed the DES to fill up the membrane pores more easily. On the contrary, as the weight percentage of LiCl increases, the DES loading decreases. This can be explained by the sponge-like microstructure and lower porosity of M-L2 and M-L3 with 61.0 and 55.9%, respectively.

Table 3 Energy dispersive X-ray (EDX) analysis of DES-supported membrane

Element	Weight percentage (%)						
	M-0	M-P1	M-P2	M-P3	M-L1	M-L2	M-L3
Carbon	50.6	37.4	38.5	30.0	48.8	52.7	51.8
Fluorine	43.3	29.8	23.9	18.4	38.2	37.3	39.4
Chlorine	5.1	12.9	17.3	21.0	5.4	4.3	4.3
Nitrogen		15.4	15.1	20.6	2.9		
Oxygen		3.2	3.9	9.3	3.6		
Silicone	1.0	1.3	1.3	0.7	1.1	5.7	4.5
Total	100	100	100	100	100	100	100

3.3 Effect of Deep Eutectic Solvents Loading on Gas Separation

The addition of a pore additive has a significant effect to the membrane performances as related to CO_2 separation. This is mainly due to the changes in the membrane morphological structures when the amount of DES loading in the membranes is varied. Pure gas permeation tests were conducted to study the gas transport properties of the supported DES membranes at 1.1 bar as a transmembrane pressure at 25°C temperature. The CO_2 and N_2 permeability and their selectivity at different pore additives ratios are shown in Figure 2.

The trend of Figure 2(a) shows that the CO_2 permeability increases with the use of a pore additive. This occurrence is suggested due to higher DES loading onto the membrane pores, assisted by the addition of PEG and LiCl as discussed in Section 3.2. For instance, the CO_2 permeability of M-P1 membrane was 2.6×10^6 Barrer, while,

the permeability of the membrane without any additional of pore additive, M-0 was only 1.5×10^6 Barrer. As for M-L1, M-L2 and M-L3 membranes with LiCl as their pore additive has demonstrated lessen improvement as compared to the membrane with PEG as pore additive. Consistently, at the same weight percentage of pore additive, it is discovered that the M-P2 permeability was 2.6×10^6 Barrer while the M-L2 permeability was only 2.1×10^6 Barrer.

This results from the dominant sponge-like structure of the M-L2 membranes, which has lowered the DES loading. In this study, it is observed that the best CO_2 permeability is 2.81×10^6 Barrer, for the M-P3 membrane, with 3 wt % of PEG. This membrane has an improvement of almost 70% in overall membrane performance as compared with the M-0 membrane without any additives. This improvement occurred such way is induced to be related by the highest porosity at 70.5% and the pores formation on the M-P3 top surface, allowing DES to fill the membrane

pores more efficiently. The higher diffusivity and solubility of CO_2 in both PVDF-co-PTFE polymer and DES is a caused by the higher permeability of CO_2 for M-P3.

In contrast, Figure 2(b) shows the effects of the pore additive ratio on the N_2 permeability. The N_2 permeability decreased from 1.3×10^6 Barrer to 8.9×10^5 Barrer and 7.3×10^5 Barrer when the PEG and LiCl weight ratios increased from 0 to 3 wt. %. This observation proves that a different DES loading has an ability in affecting the permeability of both gasses. This can be seen as higher DES loading in the M-P3 membrane has given a higher permeability of CO_2 but a lower permeability of N_2. The work of Altamash *et al.* (2020) also affirmed that differences DES loading also affecting to the performances of CO_2 sorption as per unit weight of DES available in the system. For instance, pressure below than 5 bar, the capacity of CO_2 that able to soluble in ChCl based solution was 0.5 mmol CO_2/g solvent [37]. With that, higher amount of DES loading in the membrane pores will affecting to higher amount CO_2 can be soluble and finally, separated.

The CO_2/N_2 selectivity of the synthesized supported DES membranes is featured in Figure 2(c). The selectivity is improved as the pore additive ratio increases for both PEG and LiCl. The maximum selectivity is observed at 3.16, for M-P3, which has the highest DES loading. The membrane without any additional pore formation shows the lowest selectivity, i.e., 1.18. This may be attributed by the low loading of DES in M-0 membrane pores. With lower percentage of DES found in the membrane structure via EDX analysis, the membrane structure was believed not filled up with the DES fully. Nitrogen gasses able to penetrate through the membrane freely, hence the selectivity of CO_2/N_2 is low. As shown in Figure 2(c), the incorporation of DES onto the membrane pores has improves the supported DES membrane selectivity by a factor 2.5 when 3% PEG was used as a pore additives. The same goes to supported DES membrane which also possess the highest porosity as discussed in section 3.1. The DES uptake can be further improved by the ancillary of PEG to develop the pores on top of the membrane surface with macrovoid finger-like structures.
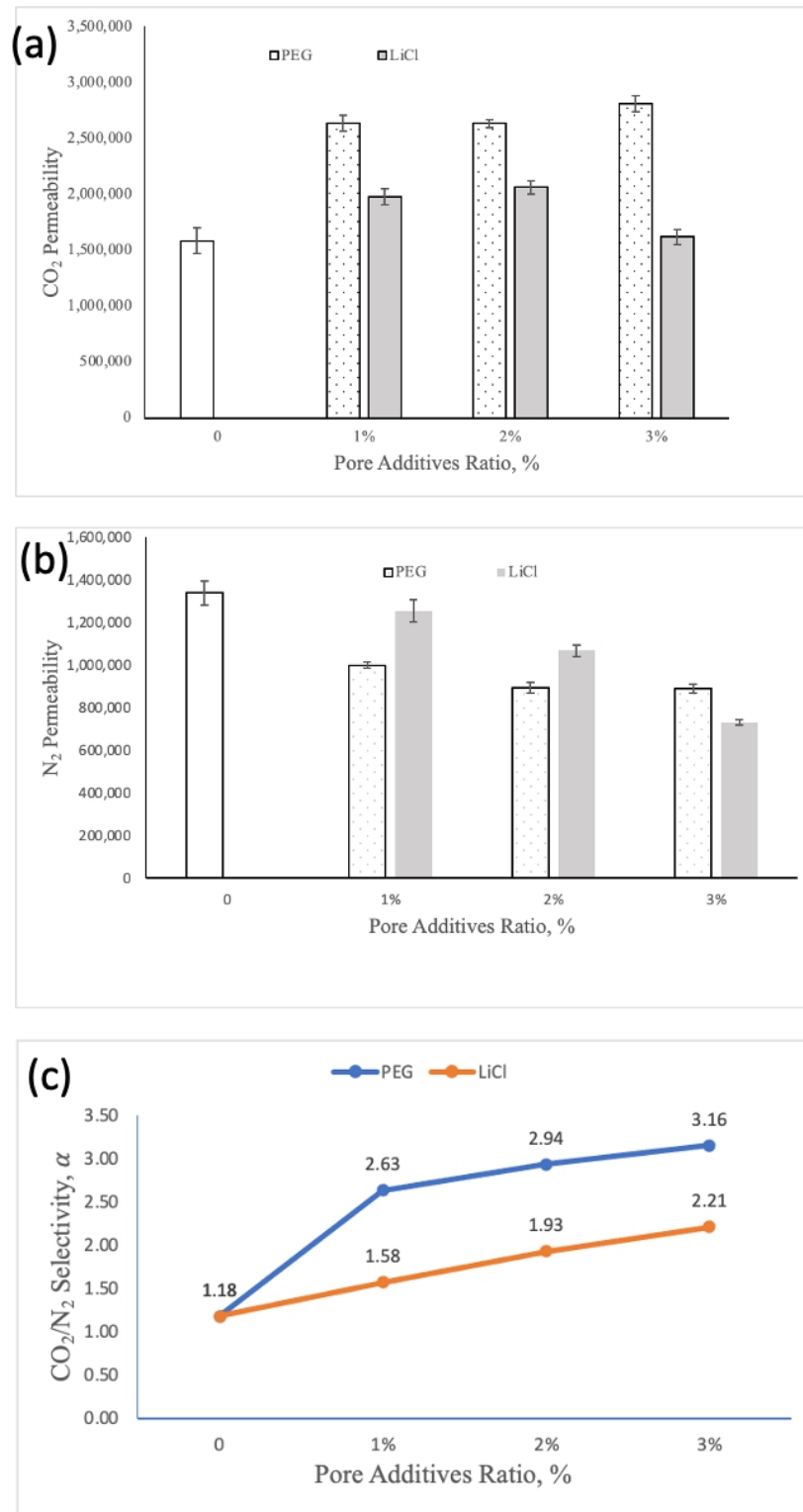
Figure 2 Effect of pore additive ratios on (a) CO_2 permeability; (b) N_2 permeability; and (c) CO_2/N_2 selectivity of supported deep eutectic solvent membranes

The revised upper bound correlation data for CO_2/N_2 separation using polymeric membranes was given by Robeson in 2008 [31]. Figure 3 illustrates the CO_2/N_2 gas separation performance of the prepared PVDF-co-PTFE membrane from different pore additives obtained in this study with others SLM results in Robeson's plot [32-35]. In general, the performance of supported-DES membranes synthesized with pore addition showed a great improvement in permeability and a slight enhancement in selectivity. The improvement was attributed by the presence of DES in the membrane pores, which has a high attraction for CO_2 as a target gas. The CO_2 permeability of M-P3 and M-P2 exceeds the upper bound curve and gives a better performance. Hence, the results demonstrate that the prepared supported DES membrane is indeed a promising candidate for separating CO_2/N_2. However, low CO_2/N_2 selectivities in all supported-DES membranes could be due to the rubbery features of PVDF-co-PTFE membranes [36].
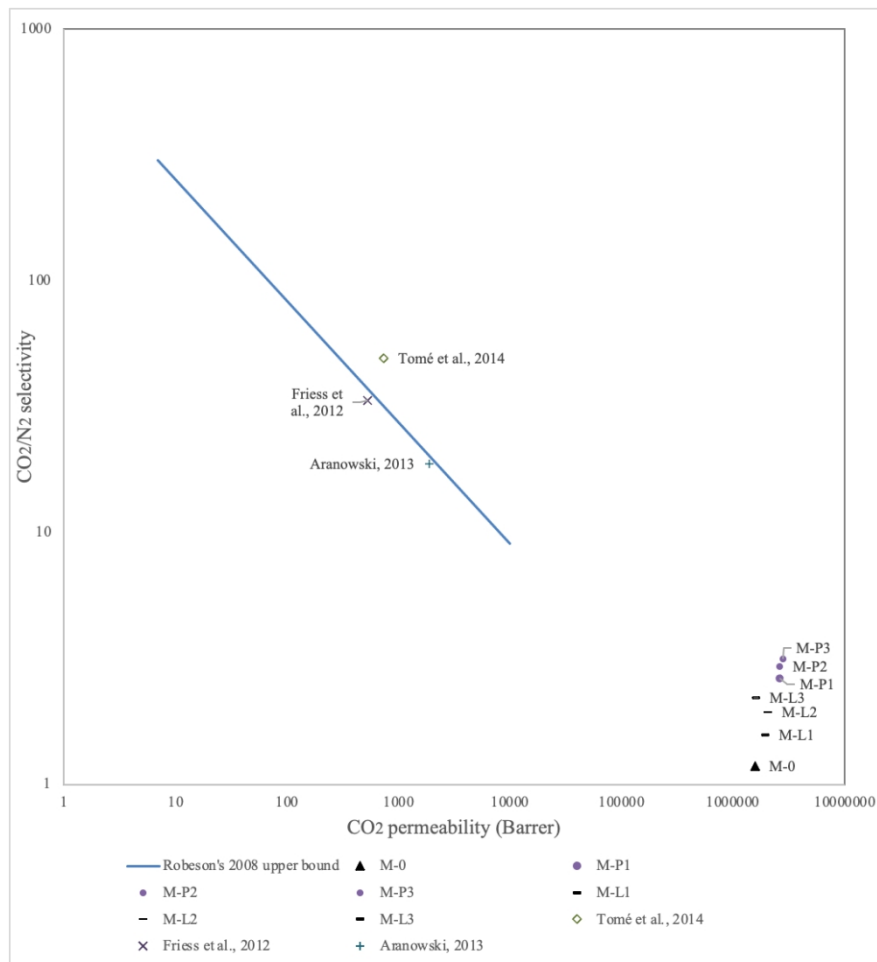

Figure 3 Comparison of CO_2/N_2 gas permeation results obtained in this study with others reported SLM in the relation to the Robeson upper limits [33-35]

4.0 CONCLUSION

In this work, seven different DES-supported membranes were successfully synthesised by using different pore additives (PEG and LiCl) at different weight percentages (1, 2 and 3 wt. %). Throughout the tests, the physical properties and gas separation performance of DES-supported membranes were established. In overall, the performance of DES-supported membranes are dependent to several factors such as; (i) level of membrane porosity (ii) type of pore additive and (iii) the ratio of pore additive in polymer solution. Indeed, the study discovered that PEG is the best pore formation agent that affects the immobilisation of DES in supported liquid membranes, whereas LiCl is best to be used as macrovoid pore reducer. Therefore, membrane used PEG as additives, has the best performance in CO_2/N_2 separation, with the highest selectivity.

ACKNOWLEDGEMENT

REFERENCES

[1]   Peters, G. P., *et al*. 2020. Carbon Dioxide Emissions Continue to Grow Amidst Slowly Emerging Climate Policies. *Nature Climate Change*. 10(1): 3-6.

[2]   Nicolas, C.-H., *et al*. 2011. Role of Adsorption and Diffusion Pathways on the CO_2/N_2 Separation Performance of Nanocomposite (B)-MFI-alumina Membranes. *Chemical Engineering Science*. 66(23): 6057-6068.

[3]   Pereira, L., and Posen, I. D. 2020. Lifecycle Greenhouse Gas Emissions from Electricity in the Province of Ontario at Different Temporal Resolutions. *Journal of Cleaner Production*. 270: 122514.

[4]   Merkel, T. C., *et al.* 2010. Power Plant Post-combustion Carbon Dioxide Capture: An Opportunity for Membranes. *Journal Of Membrane Science.* 359(1-2): 126-139.

[5]   Yu, C.-H., C.-H. Huang, and C.-S. Tan. 2012. A Review of CO_2 Capture by Absorption and Adsorption. *Aerosol Air Qual. Res.* 12(5): 745-769.

[6]   Chen, H. Z., P. Li, and T.-S. Chung. 2012. PVDF/ionic Liquid Polymer Blends with Superior Separation Performance for Removing CO_2 from Hydrogen and Flue Gas. *International Journal of Hydrogen Energy*. 37(16): 11796-11804.

[7]   Brunetti, A., *et al.* 2014. Engineering Evaluation of CO_2 Separation by Membrane Gas Separation Systems. *Journal of Membrane Science.* 454: 305-315.

[8]   Guillen, G. R., *et al.* 2011. Preparation and Characterization of Membranes Formed by Nonsolvent Induced Phase Separation: A Review. Industrial & Engineering *Chemistry Research.* 50(7): 3798-3817.

[9]   Cui, Z., E. Drioli, and Y. M. Lee. 2014. Recent Progress in Fluoropolymers for Membranes. *Progress in Polymer Science*. 39(1): 164-198.

[10]   Xiang, L., *et al.* 2017. Thin poly (ether-block-amide)/attapulgite Composite Membranes with Improved CO_2 Permeance and Selectivity for CO_2/N_2 and

CO₂/CH₄. *Chemical Engineering Science.* 160: 236-244.

[11]   Baker, R. W. 2002. Future Directions of Membrane Gas Separation Technology. *Industrial & Engineering Chemistry Research.* 41(6): 1393-1411.

[12]   Puri, P. S. 2011. Commercial Applications of Membranes in Gas Separations. *Membrane Engineering for the Treatment of Gases.* 215-244.

[13]   Asghari, M. M. Mosadegh, and H. R. Harami. 2018. Supported PEBA-zeolite 13X Nano-composite Membranes for Gas Separation: Preparation, Characterization and Molecular Dynamics Simulation. *Chemical Engineering Science.* 187: 67-78.

[14]   Dou, H., *et al*. 2019. Supported Ionic Liquid Membranes with High Carrier Efficiency Via Strong Hydrogen-bond Basicity for the Sustainable and Effective Olefin/Paraffin Separation. *Chemical Engineering Science.* 193: 27-37.

[15]   Zeng, Y., *et al*. 2018. Capture of CO₂ in Carbon Nanotube Bundles Supported with Room-temperature Ionic Liquids: A Molecular Simulation Study. *Chemical Engineering Science.* 192: 94-102.

[16]   Dai, Z., *et al*. 2016. Combination of Ionic Liquids with Membrane Technology: A New Approach for CO₂ Separation. *Journal of Membrane Science.* 497: 1-20.

[17]   Scovazzo, P., *et al*. 2002. Supported Ionic Liquid Membranes and Facilitated Ionic Liquid Membranes. *ACS Symposium Series*. American Chemical Society.

[18]   Paiva, A., *et al*. 2014. Natural Deep Eutectic Solvents–solvents for the 21st Century. *ACS Sustainable Chemistry & Engineering.* 2(5): 1063-1071.

[19]   Li, G., *et al*. 2014. Solubilities and Thermodynamic Properties of CO₂ in Choline-chloride based Deep Eutectic Solvents. *The Journal of Chemical Thermodynamics.* 75: 58-62.

[20]   Abbott, A. P., *et al*. 2011. Glycerol Eutectics as Sustainable Solvent Systems. *Green Chemistry.* 13(1): 82-90.

[21]   Feng, C., *et al*. 2004. Preparation and Properties of Microporous Membrane from Poly (Vinylidene Fluoride-Co-Tetrafluoroethylene)(F2. 4) for Membrane Distillation. *Journal of Membrane Science.* 237(1): 15-24.

[22]   Constantin, V., A. K. Adya, and A. -M. Popescu. 2015. Density, Transport Properties and Electrochemical Potential Windows for the 2-hydroxy-N, N, N-trimethylethanaminium Chlorides Based Ionic Liquids at Several Temperatures. *Fluid Phase Equilibria.* 395: 58-66.

[23]   Ahmad, A., *et al*. 2012. Effect of Ethanol Concentration in Water Coagulation Bath on Pore Geometry of PVDF Membrane for Membrane Gas Absorption Application in CO₂ Removal. *Separation and Purification Technology.* 88: 11-18.

[24]   Wang, Q., Z. Wang, and Z. Wu. 2012. Effects of Solvent Compositions on Physicochemical Properties and Anti-fouling Ability of PVDF Microfiltration Membranes for Wastewater Treatment. *Desalination.* 297: 79-86.

[25]   Li, Q., Z. L. Xu, and L.Y. Yu, 2010. Effects of Mixed Solvents and PVDF Types on Performances of PVDF Microporous Membranes.

Journal of Applied Polymer Science. 115(4): 2277-2287.

[26] Aroon, M., *et al.* 2010. Morphology and Permeation Properties of Polysulfone Membranes for Gas Separation: Effects of Non-solvent Additives and Co-solvent. *Separation and Purification Technology.* 72(2): 194-202.

[27] Fontananova, E., *et al.* 2006. Effect of Additives in the Casting Solution on the Formation of PVDF Membran*es. Desalination.* 192(1-3): 190-197.

[28] Salleh, W. and A. F. Ismail. 2015. Carbon Membranes for Gas Separation Processes: Recent Progress and Future Perspective. *Journal of Membrane Science and Research.* 1: 2-15.

[29] Alamery, H. R. D., M. I. Hatim, and M. S. Ahmad. 2016. A Study of the Effects of Adding PEG on the Properties and Morphology of Asymmetric Membranes Comprising PVDF-HFP co-Polymer Fabricated by Phase Inversion Method. *ARPN J. Eng. Appl. Sci.* 11(11): 7130-7140.

[30] Mansourizadeh, A., *et al.* 2010. Preparation of Polyvinylidene Fluoride Hollow Fiber Membranes for CO_2 Absorption Using Phase-inversion Promoter Additives. *Journal of Membrane Science.* 355(1): 200-207.

[31] Robeson, L. M. 2008. The Upper Bound Revisited. *Journal of Membrane Science.* 320(1-2): 390-400.

[32] Luis, P. and B. Van der Bruggen, 2013. The Role of Membranes in Post-combustion CO_2 Capture. *Greenhouse Gases: Science and Technology.* 3(5): 318-337.

[33] Friess, K., *et al.* 2012. High Ionic Liquid Content Polymeric Gel Membranes: Correlation of Membrane Structure with Gas and Vapour Transport Properties. *Journal of Membrane Science.* 415: 801-809.

[34] Tomé, L. C., *et al.* 2014. Playing with Ionic Liquid Mixtures to Design Engineered Co_2 Separation Membranes. *Physical Chemistry Chemical Physics.* 16(32): 17172-17182.

[35] Aranowski, R. 2013. Influence of Ionic Liquid Structure on Supported Ionic Liquid Membranes Effectiveness In Carbon Dioxide/Methane Separation. *Journal of Chemistry.*

[36] Mannan, H., *et al.* 2017. Synthesis, Characterization, and CO_2 Separation Performance of Polyether Sulfone/[EMIM][Tf2N] Ionic Liquid-Polymeric Membranes (ILPMs). *Journal of Industrial and Engineering Chemistry.* 54: 98-106.

[37] Altamash, T., *et al.* 2020. Effect of Hydrogen Bond Donors and Acceptors on CO_2 Absorption by Deep Eutectic Solvents. *Processess.* 8(12): 1533

[38] Plotka-Wasylka, J., *et al.* 2020. Deep Eutectic Solvents vs Ionic Liquids: Similarities and Differences. *Microchemical Journal.* 105539.